AIAA 2002-0368
Mach Wave Elimination Applied to Turbofan Engines

D. Papamoschou
Dept. of Mechanical & Aerospace Engineering
University of California, Irvine
Irvine, CA

M. Debiasi
Dept. of Mechanical Engineering
Ohio State University
Columbus, OH

40th Aerospace Sciences Meeting & Exhibit
14-17 January 2002
Reno, Nevada

AIAA-2002-0368

MACH WAVE ELIMINATION APPLIED TO TURBOFAN ENGINES

Dimitri Papamoschou *
University of California, Irvine, Irvine, California 92697-3975
and
Marco Debiasi †
Ohio State University, Columbus, Ohio 43235

This is a joint thermodynamic and acoustic study of engines for next-generation supersonic aircraft. It explores fixed-cycle concepts with potential for quiet takeoff and efficient cruise. The flow path is clean, without mechanical suppressors. The strategy is to take a representative state-of-the-art military turbofan engine and increase its bypass ratio to moderate value. The engine core stays the same. Three exhaust configurations are considered: mixed flow, coaxial separate flow, and eccentric separate flow. Engine cycle analysis predicts thermodynamic performance and nozzle exhaust conditions at takeoff and Mach 1.6 cruise. Subscale experiments duplicate the exhaust conditions at takeoff and measure the far-field sound. Flyover perceived noise levels are estimated for a twin-engine aircraft in the 120000-lb class. The eccentric arrangement is 6 dB quieter than the mixed-flow arrangement and 5 dB quieter than the coaxial configuration. Spectral and time-domain analyses indicate that the eccentric exhaust is free of strong Mach wave radiation. The acoustic benefit of the eccentric arrangement, combined with faster climb afforded by the modified engine, leads to a reduction of 14 dB in effective perceived noise level. Compared to the baseline engine, the specific fuel consumption of the modified engine is about 20% less at subsonic speeds and 3% less at supersonic cruise.

Nomenclature

D	=	diameter
f	=	frequency
$\dot{m}$	=	mass flow rate
M	=	Mach number
U	=	velocity
r	=	distance from jet exit
t	=	time from lift off
$\mathcal{T}$	=	thrust
x	=	horizontal distance from brake release
y	=	altitude
α	=	geometric angle of attack
γ	=	climb angle
θ	=	polar angle relative to jet centerline
ϕ	=	azimuth angle relative to vertical plane
ψ	=	polar observation angle of airplane

Subscripts

com	=	compressor
eng	=	full-scale engine
exp	=	subscale experiment
fan	=	fan tip
LO	=	lift off
p	=	primary (core) exhaust
s	=	secondary (bypass) exhaust
TOM	=	takeoff monitor
tot	=	total
∞	=	flight conditions

Abbreviations

BPR	=	Bypass Ratio
EPNL	=	Effective Perceived Noise Level
FPR	=	Fan Pressure Ratio
PNL	=	Perceived Noise Level
PNLM	=	Maximum value of PNL
SPL	=	Sound Pressure Level
OASPL	=	Overall Sound Pressure Level
OPR	=	Overall Pressure Ratio
TIT	=	Turbine Inlet Temperature
TSFC	=	Thrust Specific Fuel Consumption

*Professor, Associate Fellow AIAA
†Post Doctoral Researcher, member AIAA

Introduction

Community noise from aircraft has profound environmental and economic consequences. First-generation subsonic jetliners were very noisy because of the high exhaust velocity of their engines. Efforts to suppress noise using mixing enhancement had only moderate impact [1]. It wasn't until the introduction of the high-bypass-ratio turbofan that noise was reduced remarkably, by 20-30 decibels. This was achieved by the simple fact that the same thrust was produced with a larger mass flow rate, hence lower exhaust speed. The associated gains in propulsive efficiency led to much lower fuel consumption, making the high-bypass turbofan the only choice for commercial aircraft developed in the 1980s and beyond. The increase in bypass ratio was enabled by development of high-temperature materials for the turbine blades. For given size of the gas generator, the power that can be delivered to the bypass stream is directly related to the turbine inlet temperature (TIT).

Development of economically viable supersonic transports hinges on solving the problem of community noise without penalizing aircraft performance. The same issue affects to some extent military high-performance aircraft as communities surrounding military bases are becoming increasingly sensitive to noise. So far, the bulk of the supersonic noise suppression effort has encompassed mixing enhancement and ejector approaches [2, 3] which typically lead to large and heavy powerplants [4]. One may wonder if supersonic engines will follow the same evolution as subsonic engines, leading to supersonic high-bypass turbofans. The issue is not as simple, though. High bypass ratio generally causes worse, not better efficiency at supersonic speeds. Figure 1 shows calculations of thrust specific fuel consumption (TSFC) and fan diameter versus bypass ratio (BPR) and fan pressure ratio (FPR) at cruise Mach number of 1.6. The calculation, based on an engine cycle analysis mentioned later in the paper, assumes TIT=1600°K (2400°F), a value close to today's limits of turbine materials. It is seen that the TSFC slightly dips and then rises with increasing bypass ratio. The fan diameter increases roughly with $\sqrt{1+\mathrm{BPR}}$ meaning increased drag and weight of the vehicle. The quantitative information shown in Fig. 1 will change somewhat with the assumptions of the cycle analysis (e.g., component efficiencies) but the qualitative trends will not. It is obvious form the graphs that bypass ratios beyond 3.0 would lead to very poor performance at supersonic cruise.

Designers of supersonic engines, therefore, face two

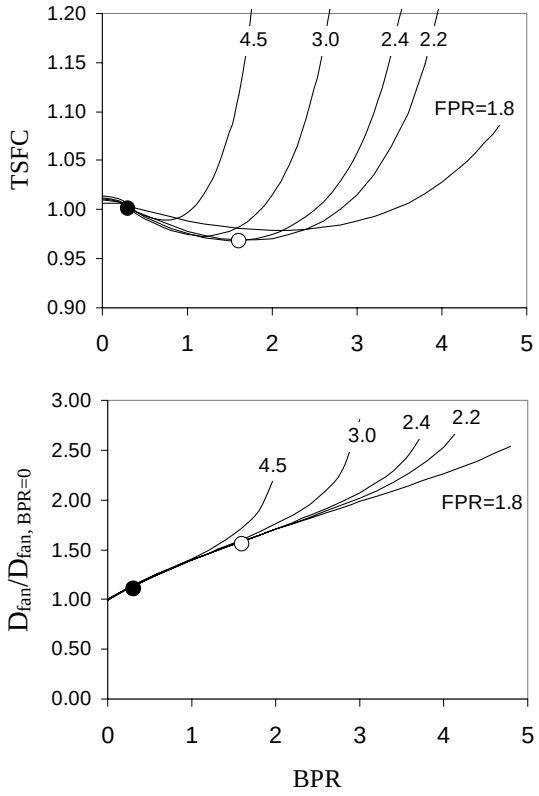

Fig.1 Thrust specific fuel consumption and fan diameter, normalized by turbojet value, versus bypass ratio and fan pressure ratio for Mach 1.6 cruise. Solid and open symbols indicate the baseline and modified engines of this study, respectively.

conflicting requirements: high bypass ratio on take-off/landing for reduced noise and low–or zero–bypass ratio for efficient supersonic cruise. One possibility is the variable-cycle turbofan engine, but it entails complexity far greater than that of today's engines. Another approach is to seek an intermediate bypass ratio that satisfies both requirements in a fixed cycle. Since the bypass ratio would be moderate, it becomes crucial how one uses the bypass stream to reduce noise. One configuration is the mixed-flow turbofan, currently used on all military engines, in which the bypass and core streams mix before exiting a common nozzle. The other option is the separate (unmixed)-flow turbofan, which is very common on subsonic transports. The unmixed design allows shaping of the bypass exhaust so that the bypass stream substantially shields noise emitted from the core stream. Previous work on the Mach Wave Elimination (MWE) technique showed significant gains in noise reduction by changing the shape of a dual-stream exhaust from coaxial to eccentric [5].

Mach wave radiation is considered the principal source of mixing noise in supersonic jets [6]-[11]. It could also play a strong role in noise emission from high-subsonic jets due to the growth-decay nature of instability waves, which creates a spectrum of phase speeds part of which is supersonic [12, 13]. In the MWE method, generation of Mach waves from a primary stream is suppressed by flowing a secondary parallel stream adjacent to the primary stream so that all relative eddy motions become subsonic [14]. Specifically, MWE seeks to minimize the convective Mach numbers of turbulent eddies throughout the jet flow field. This includes the end of the potential core, a region of vigorous mixing and strong noise generation. In a coaxial arrangement, application of the secondary flow reduces the growth rate of the shear layer between the primary and secondary streams, thus stretching the primary potential core. The end of the primary potential core can easily extend past the reach of the secondary flow, thus reducing the effectiveness of the technique. The eccentric arrangement has been shown to prevent significant elongation of the primary potential core [15]. It also doubles the thickness and potential core length of the secondary flow in the downward direction, thus making the technique very effective at suppressing Mach wave emission towards the ground. More generally, the MWE results illustrate the potential for noise reduction by shaping the mean flow of the primary and secondary streams. Our study represents the initial steps of a broader effort to reduce supersonic and subsonic jet noise by mean profile shaping of realistic engine flows.

This paper examines, at a fundamental level, the thermodynamic and acoustic performance of a fixed-cycle, moderate-bypass supersonic engine. It will be shown that significant noise reduction relative to today's military turbofan engines is achievable with an eccentric separate-flow exhaust that shields noise from the core stream.

Engine Configurations

We consider a supersonic twin-engine aircraft with maximum take-off weight of about 540 kN (120,000 lb.) The assumed lift-to-drag ratio is 5 at takeoff and 10 at supersonic cruise, values roughly 20% better than those of the Aerospatiale Concorde [16]. The study starts with a representative military turbofan engine for this kind of airplane, increases its bypass ratio to moderate value, and assesses noise and performance of three configurations: the mixed-flow turbofan; the separate-flow turbofan with coaxial exhaust; and the separate-flow turbofan with eccentric exhaust. The comparison basis is the following:

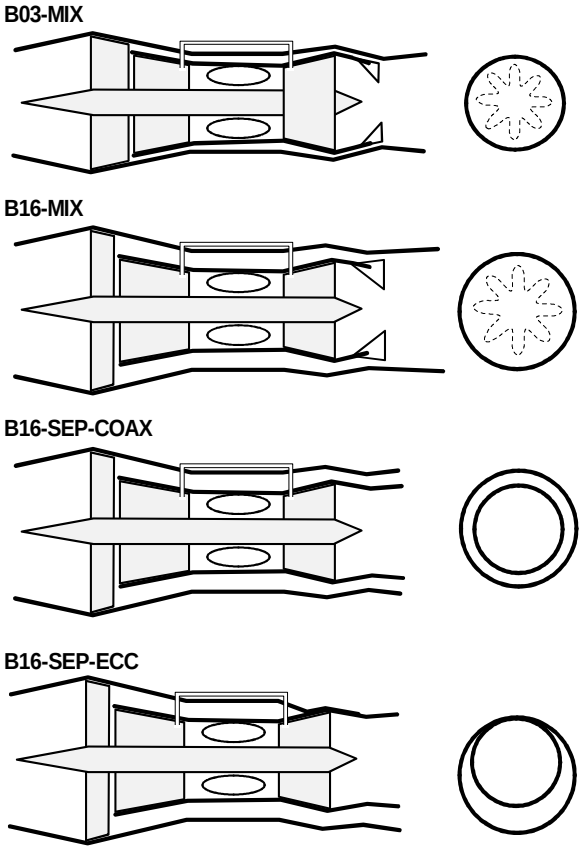

Fig.2 Engine designs.

(a) All engines have the same supersonic cruise thrust.

(b) All engines have the same core characteristics (mass flow rate, overall pressure ratio, turbine inlet temperature).

The baseline engine is a military turbofan with BPR=0.3, FPR=5.0, static thrust of 126 kN (28000 lb) and cruise thrust of 30 kN (6700 lb) at Mach 1.6 and altitude of 16000 m. The static thrust is dictated by the ability of the aircraft to climb with only one engine operating. The modified engines are increased mass flow rate derivatives of the baseline engine, with bypass ratio 1.6. The size, specific fuel consumption, and exhaust conditions of the engines is derived from thermodynamic analysis of a Brayton cycle with component efficiencies and specific heat ratios listed in Table 1 (see Ref. [18] for more information on the cycle analysis.) For all engines,

Table 1: Engine Cycle Assumptions

Component	Efficiency	Specific heat ratio
Inlet ($M_\infty < 1$)	0.97	1.40
Inlet ($M_\infty \geq 1$)	0.85	1.40
Fan	0.85	1.40
Compressor	0.85	1.37
Combustor	1.00[1]	1.35
Turbine	0.90	1.33
Nozzle	0.97	calc.[2]

(1) With 5% total pressure loss
(2) From internal mixing calculation

Table 2: Engine Characteristics at Takeoff
($y = 0$ m, $M_\infty = 0$)

	B03-MIX	B16-SEP	B16-MIX
OPR	30	30	30
TIT[1] (K)	1800	1800	1800
$\dot{m}_{\text{com}}$ (kg/s)	125	120	115
$\dot{m}_{\text{tot}}$ (kg/s)	160	303	290
$\mathcal{T}$ (kN)	126	162	159
BPR	0.30	1.60	1.60
FPR	5.0	2.6	2.6
$D_{\text{fan}}^{(2)}$ (m)	1.04	1.43	1.40
TSFC (kg/kgf-h)	0.67	0.50	0.49[3]
M_p	1.55	1.20	1.20
U_p (m/s)	770	640	530
M_s	-	1.20	-
U_s (m/s)	-	430	-

(1) 30% compressor flow for turbine blade cooling
(2) $M = 0.5$ at fan face
(3) Does not account for mixer losses

Table 3: Engine Characteristics at Cruise
($y = 16000$ m, $M_\infty = 1.6$)

	B03-MIX	B16-SEP	B16-MIX
OPR	24	24	24
TIT[1] (K)	1600	1600	1600
$\dot{m}_{\text{com}}$ (kg/s)	55	53	51
$\dot{m}_{\text{tot}}$ (kg/s)	72	137	131
$\mathcal{T}$ (kN)	30	30	30
BPR	0.3	1.6	1.6
FPR	4.5	2.2	2.2
$D_{\text{fan}}^{(2)}$ (m)	1.04	1.43	1.40
TSFC (kg/kgf-h)	1.00	0.97	0.94[3]
M_p	2.10	1.80	1.90
U_p (m/s)	890	820	700
M_s	-	1.95	-
U_s (m/s)	-	610	-

(1) 25% compressor flow for turbine blade cooling
(2) $M = 0.7$ at fan face
(3) Does not account for mixer losses

25-30% of the compressor air is used for turbine cooling; 1% of the compressor air is bled to systems outside the engine; and 1.5% of the turbine work drives auxiliary systems. Total pressure loss due to turbine cooling is estimated at 7% times the mass fraction of cooling air [17]. For the mixed-flow design, the core and fan streams mix at constant pressure, constant total enthalpy, and Mach number 0.4 before expanding to ambient pressure. The OPR and TIT for maximum static thrust were selected at 30 and 1800°K, respectively. The requirement that all engines have the same supersonic cruise thrust sets the size of each engine. Specifically, it makes the fan diameter of each engine dependent on the OPR and TIT chosen for cruise. Since the fan diameter is a constant throughout the aircraft mission, the OPR and TIT values at cruise define the static thrust. They were chosen such that the baseline (smallest) engine provides enough thrust for climb with one engine inoperative, i.e., $\mathcal{T}$ =126 kN.

The engine configurations are summarized in Fig. 2. For convenience, we adopt a notation that gives the bypass ratio and type of exhaust. B16-MIX, for example, describes the bypass ratio 1.6, mixed-flow engine. The suffixes COAX and ECC indicate a coaxial or eccentric exhaust, respectively, of the separate-flow engine. For the eccentric configuration, an additional numerical suffix indicates the azimuth angle at which noise was measured. Tables 2 and 3 summarize engine characteristics and thermodynamic performance at takeoff and supersonic cruise, respectively. Exhaust conditions are pressure matched. Due to their increased mass flow rate, the modified engines have 28% higher static thrust than the baseline engine. The takeoff fan pressure ratio of the modified engines is 2.6, a value that presently may require a two-stage fan but in the future may be achievable with a single-stage aspirated fan [19]. At takeoff, the thrust specific fuel consumption (TSFC) of the modified engines is 25% lower than that of the baseline engine. Calculations for Mach 0.8 cruise, not presented here, show a 15% improvement in TSFC. At supersonic cruise, the TSFCs of the modified engines are marginally lower than that of the baseline engine. As mentioned in the introduction, increased bypass ratio at supersonic cruise yields only small benefits in fuel consumption. The mixed-flow turbofan has slightly better fuel consumption than the separate flow turbofan. This calculation, however, does not include mixer losses or the added weight of the internal mixer on overall engine performance. The velocity ratio of the separate-flow exhaust at cruise, $U_s/U_p = 0.74$, is very close to the efficiency of energy transfer between the core and

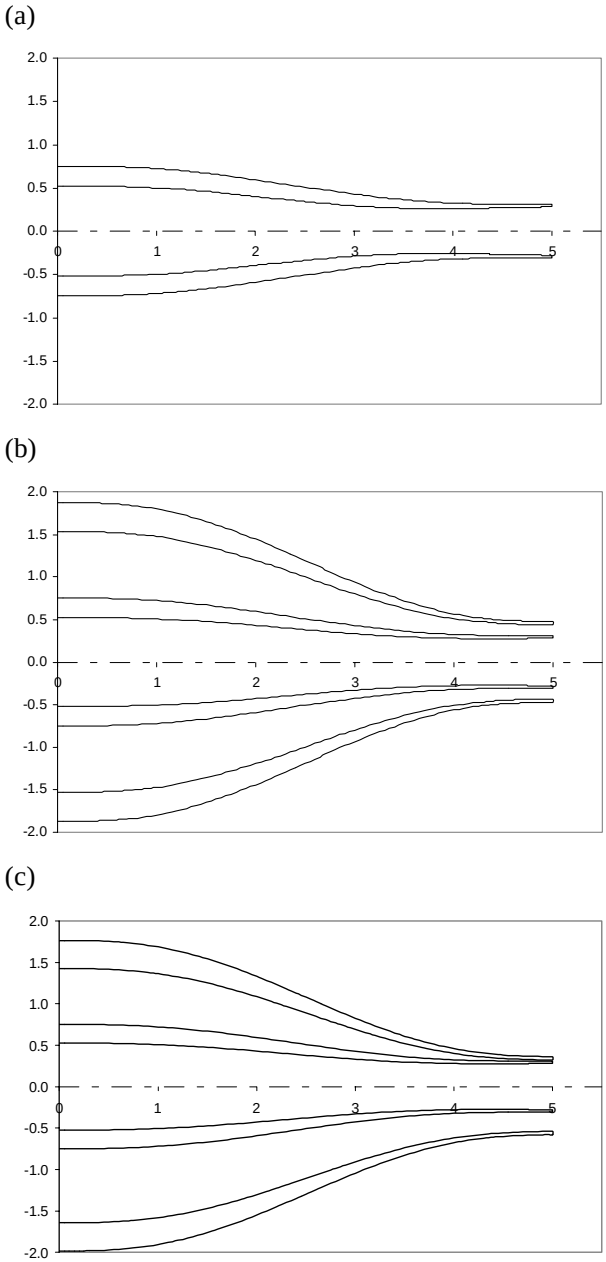

Fig.3 Nozzle coordinates (inches) for (a) B03-MIX; (b) B16-SEP-COAX; and (c) B16-SEP-ECC-0. The nozzle for B16-MIX was the inner one alone of (b)/(c).

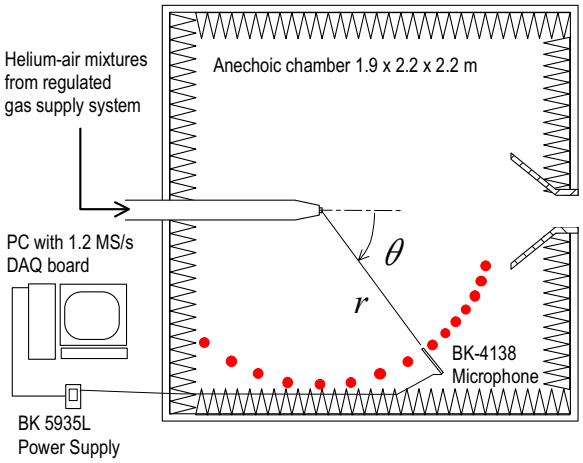

Fig.4 Experimental setup with set of polar angles covered.

bypass flow (the product of turbine and fan efficiencies, in this case 0.76). This indicates that B16-SEP operates at optimal cruise conditions [20].

Noise Measurement

Facilities

Noise testing was conducted in UCI's Jet Aeroacoustics Facility [5]. Single- and dual-stream jets with flow conditions matching those given by the cycle analysis (Table 2) were produced. The jets were composed of helium-air mixtures, which duplicate very accurately the fluid mechanics and acoustics of hot jets [21]. Jet nozzles were fabricated from epoxy resin using rapid-prototyping techniques. Two primary (core) nozzles were designed with the method of characteristics for Mach numbers 1.5 and 1.2, matching approximately the takeoff exit Mach numbers of the baseline and modified engines, respectively. Both primary nozzles had the same exit inner diameter (14.8 mm), lip thickness (0.7 mm), and external shape. One secondary (bypass) nozzle formed a convergent duct in combination with the primary nozzle and terminated in a diameter of 21.8 mm. The pipe that fed the primary nozzle was able to flex, enabling coaxial or eccentric secondary flow passages. Figure 3 plots the coordinates of the nozzles. For all nozzles, the radial coordinates of the contraction (prior to any supersonic expansion) were given by fifth-order polynomials. The contraction ratio was 4:1 for the core nozzles and 15:1 for the bypass nozzle. The jet Reynolds number was on the order of 0.5×10^6.

Noise measurements were conducted inside an anechoic chamber using a one-eighth inch condenser microphone (Brüel & Kjær 4138) with frequency response of 140 kHz. The microphone was mounted on a pivot arm and traced a circular arc centered at the jet exit with radius of 71 core jet diameters. Earlier experiments have determined that this distance is well inside the acoustic far field [23]. The polar angle θ ranged from 20° to 130° in intervals of 5° for $20° \leq \theta \leq 50°$ and 10° for the rest. Figure 4 shows the overall setup and the range of polar angles covered. For the eccentric jet, azimuth angles $\phi = 0°$ and 45° were investigated. The sound spectra were corrected for the microphone frequency response, free field response, and atmospheric absorption. All spectra are referenced to r/D_p=100. Comparison at equal thrust is done using geometric scaling [23].

Spectra

Sound pressure level spectra are compared at equal thrust $\mathcal{T} = 50$ N unless otherwise noted. A frequency range of great relevance to perceived noise level is 25-75 kHz, which on a full-scale engine corresponds roughly to 500-1500 Hz. Below this range, the human ear becomes insensitive to noise; above this range, sound gets attenuated very rapidly by atmospheric absorption.

Figure 5 compares the spectra of B03-MIX, B16-MIX, and B16-SEP-ECC-0 at their respective angles of peak noise emission (aft quadrant). The eccentric, separate-flow case has dramatically lower noise levels than the baseline case: about 8-dB reduction at low frequencies and 20-dB reduction at moderate-to-high frequencies. The mixed-flow case is much louder than the separate-flow eccentric case, its spectrum exceeding that of B16-SEP-ECC-0 by 2-3 dB at $f < 5$ kHz, 8 dB at $f \approx 10$ kHz, and 10-12 dB for $f > 20$ kHz. It should be noted that an actual mixed-flow exhaust would be noisier that that shown here due to exit non-uniformities and internal noise from mixing. Figure 6 compares the spectra of B03-MIX, B16-SEP-CORE (core stream alone), B16-SEP-COAX, B16-SEP-ECC-0, and B16-SEP-ECC-45. The core stream of the modified engine is almost as loud as the exhaust of the baseline engine, except at very low frequencies where it is about 3 dB quieter. The reduction in exhaust velocity from 770 m/s to 640 m/s did not bring appreciable noise reduction. The separate-flow, coaxial exhaust is on average 6-8 dB louder than the eccentric exhaust. The spectra of the eccentric case at azimuth angles

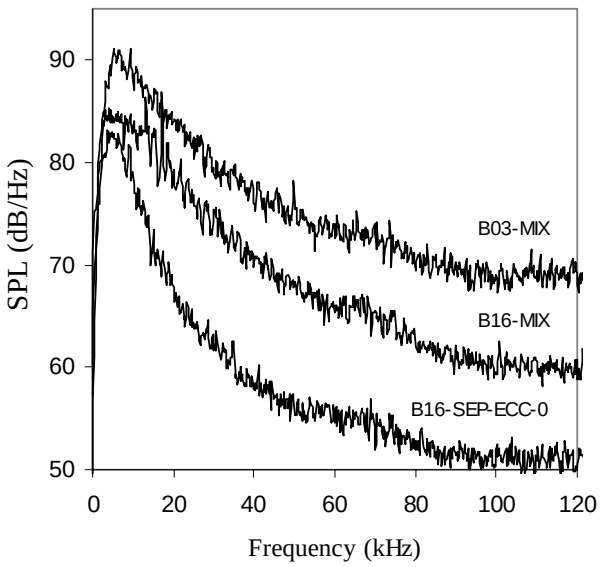

Fig.5 Far-field spectra in the direction of peak emission and scaled to equal thrust: baseline engine (B03-MIX, $\theta = 40^\circ$); modified mixed-flow engine (B16-MIX, $\theta = 25^\circ$); and modified separate-flow engine with eccentric exhaust, measured at zero azimuth angle (B16-SEP-ECC-0, $\theta = 40^\circ$).

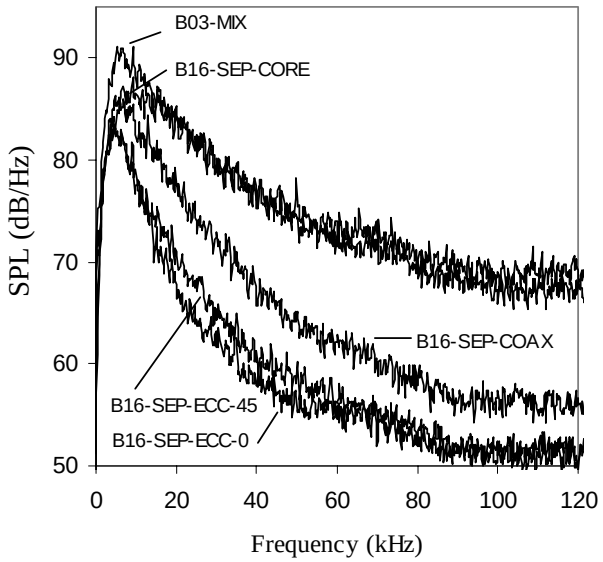

Fig.6 Far-field spectra in the direction of peak emission ($\theta = 40^\circ$ for all spectra shown) and scaled to equal thrust: baseline engine (B03-MIX); core stream only of modified separate-flow engine (B16-SEP-CORE); modified separate-flow engine with coaxial exhaust (B16-SEP-COAX); and modified separate-flow engines with eccentric exhaust, measured at zero and 45° azimuth angles (B16-SEP-ECC-0, B16-SEP-ECC-45).

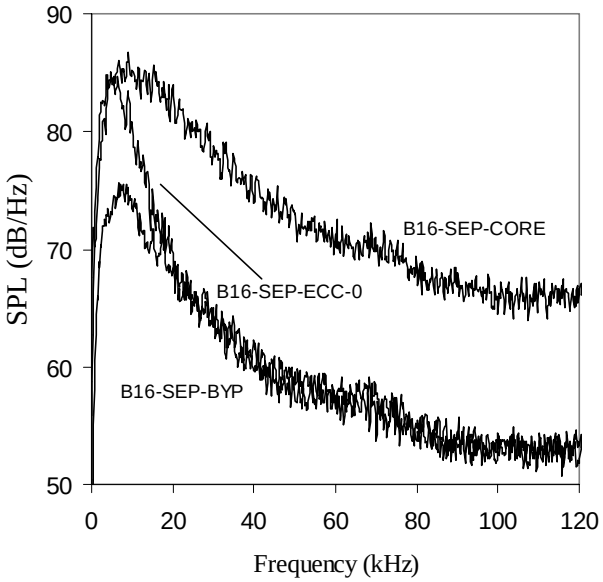

Fig.7 Far-field spectra in the direction of peak emission ($\theta = 40^\circ$ for all spectra shown), not scaled to equal thrust: core stream only of modified separate-flow engine (B16-SEP-CORE); eccentric bypass stream only of modified separate-flow engine (B16-SEP-BYP); and modified separate-flow engine with eccentric exhaust measured at zero azimuth angle (B16-SEP-ECC-0).

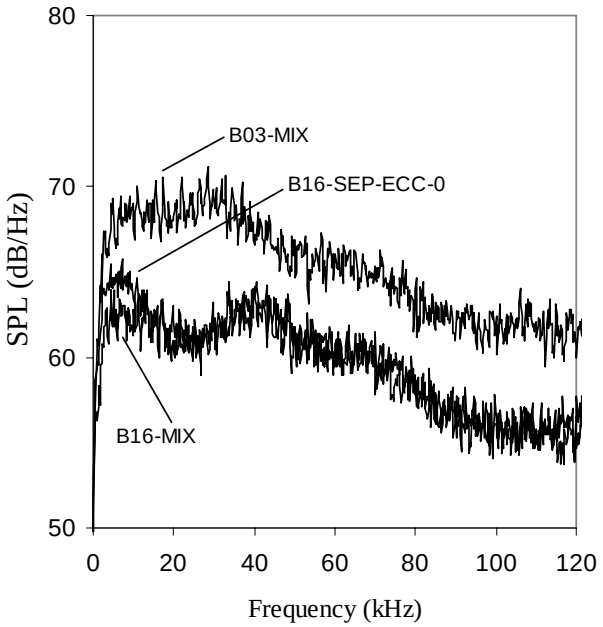

Fig.8 Far-field spectra at $\theta = 90^\circ$: baseline engine (B03-MIX); modified mixed-flow engine (B16-MIX); and modified separate-flow engine with eccentric exhaust, measured at zero azimuth angle (B16-SEP-ECC-0).

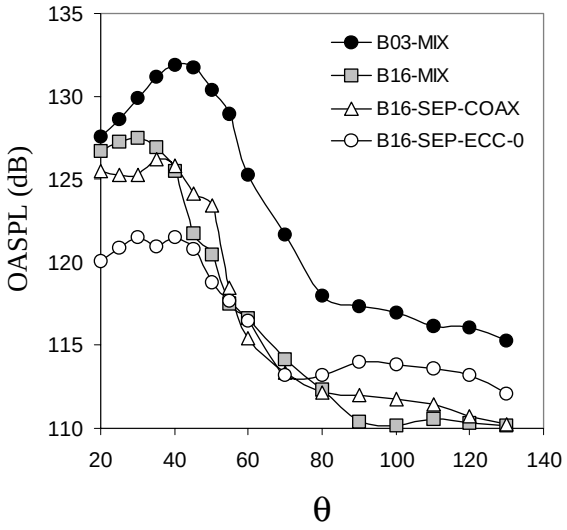

Fig.9 Directivity of overall sound pressure level for: baseline engine (B03-MIX); modified mixed-flow engine (B16-MIX); modified separate-flow engine with coaxial exhaust (B16-SEP-COAX); and modified separate-flow engine with eccentric exhaust, measured at zero azimuth angle (B16-SEP-ECC-0).

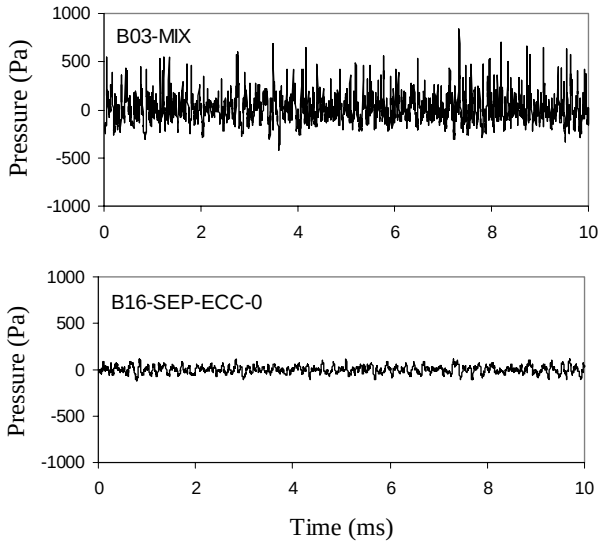

Fig.10 Microphone time traces in the direction of peak emission for baseline engine (B03-MIX) and modified separate-flow engine with eccentric exhaust, measured at zero azimuth angle (B16-SEP-ECC-0).

$\phi = 0°$ and $45°$ practically coincide, indicating that the eccentric configuration has good sideline benefit. Figure 7 presents the spectra of B16-SEP-CORE, B16-SEP-BYP (eccentric bypass stream alone), and B16-SEP-ECC-0. The spectra are presented without equal-thrust scaling to get a clearer picture of the modification of acoustic sources. Due to its lower velocity, the fan stream is much quieter than the core stream. At frequencies above 20 kHz, the spectra of B16-SEP-ECC-0 and B16-SEP-BYP coincide, that is, the combined flow emits the same noise as the bypass stream alone. This indicates that the core stream has been shielded acoustically so well that it is practically silent compared to the bypass stream, and that the bypass stream now constitutes the noise "floor." The effect of forward flight should lower this floor as the relative velocity of the bypass stream will reduce from 430 m/s to about 310 m/s at climb speed. Figure 8 shows the spectra in the lateral direction. The modified engines are 6-8 dB quieter than the baseline engine. No significant differences are noted among the modified variants.

OASPL and Skewness

Figure 9 plots the directivity of overall sound pressure level (OASPL) for B03-MIX, B16-MIX, and B16-SEP-ECC-0. The benefit of the separate-flow,

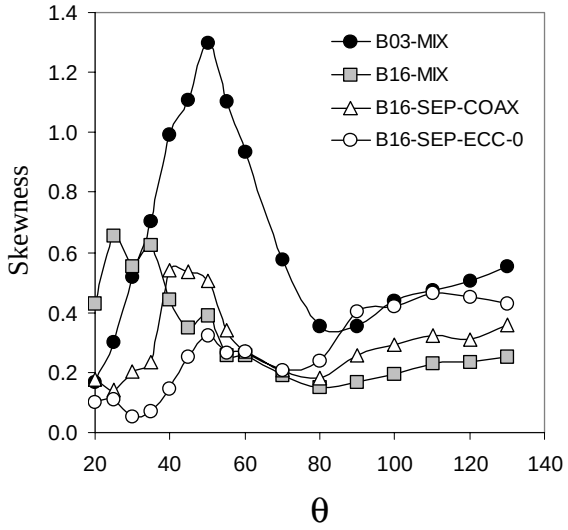

Fig.11 Directivity of normalized skewness for: baseline engine (B03-MIX); modified mixed-flow engine (B16-MIX); modified separate-flow engine with coaxial exhaust (B16-SEP-COAX); and modified separate-flow engine with eccentric exhaust, measured at zero azimuth angle (B16-SEP-ECC-0)

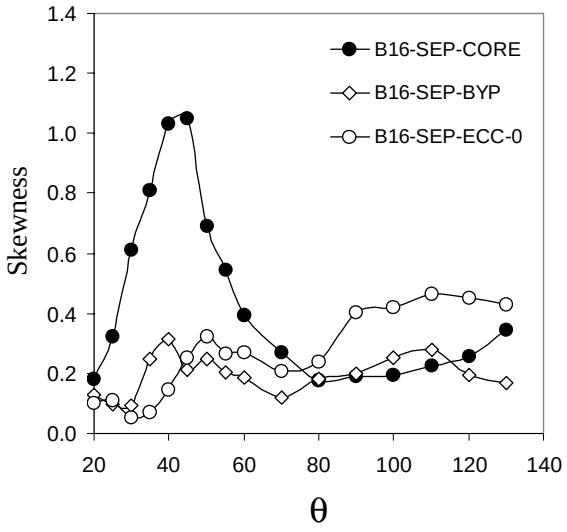

Fig.12 Directivity of normalized skewness for: core stream only of modified separate-flow engine (B16-SEP-CORE); eccentric bypass stream only of modified separate-flow engine (B16-SEP-BYP); and modified separate-flow engine with eccentric exhaust measured at zero azimuth angle (B16-SEP-ECC-0).

eccentric exhaust is again evident. To gain further insight into the modification of the noise sources, we examine the acoustic signal in time domain. Figure 10 plots the time traces of B03-MIX and B16-SEP-ECC-0 at the angle of peak emission. The signal of B03-MIX is highly skewed on the positive side and exhibits strong, irregularly-spaced positive spikes. This phenomenon is associated with nonlinear formation of Mach waves in the vicinity of the source and, in a full-scale engine, is heard as "crackle" [24]. The signal of B16-SEP-ECC-0, on the other hand, is nearly symmetric without any spikes. The normalized skewness of the asouctic signal allows quantification of this feature of noise which cannot be captured by spectral analysis. High skewness, above 0.4, is associated with emission of strong Mach waves [5, 24]. Figure 11 plots the directivity of skewness for B03-MIX, B16-MIX, B16-SEP-COAX, and B16-SEP-ECC-0. The skewness of the baseline case (B03-MIX) is very high, about 1.3, at the angle of peak emission. The skewness of the mixed-flow and coaxial-exhaust cases is substantial, exceeding the threshold of 0.4. This indicates that both of these cases emit significant Mach wave radiation. The skewness of B16-SEP-ECC-0 is very low, consistent with elimination of Mach waves. It is also instructive to compare the streams of B16-SEP-ECC separately and in combination. As shown in Fig. 12, the skewness of the core stream alone is very large, reaching 1.05 at $\theta = 45°$. The skewnesses of the bypass stream alone and of the combined flow are both very low, indicating that neither flow emits strong Mach waves. This is further evidence that Mach wave emission from the core stream has been substantially prevented by the eccentric bypass flow.

Perceived Noise Level

The regulatory definition of a quiet airplane is deceptively simple. To be able to operate, an airplane must not exceed certain noise thresholds at three set locations: takeoff, sideline, and approach. Noise is quantified in terms of the Effective Perceived Noise Level (EPNL), a metric that incorporates human annoyance to sound and its duration [22]. EPNL thresholds are based on the configuration and weight of the airplane and stem from a mix of scientific and political considerations. As the ultimate goal of this research is development of quieter airplanes, it is essential to obtain estimates of perceived full-scale noise. Here we attempt to process our spectra into EPNL for obtaining an assessment of perceived noise *reduction*. The absolute levels of EPNL will not be accurate as the effect of forward flight on jet acoustics was not present in the experiments. We calculate noise recorded from the takeoff monitor for a full-power takeoff. Future studies will address takeoff with power cutback and noise monitored from the sideline and approach monitors.

Flight Path

The first step in assessing perceived noise is definition of the takeoff flight path and attitude of the engines relative to the flight path. The airplanes are those defined in the Engine Configuration section, i.e., twin-engine with thrust given by the specifications of Table 2. The flight path of the baseline aircraft comprises a takeoff roll $x_{\text{LO}} = 1800$ m followed by a straight climb at angle $\gamma = 15°$. The lift coefficient at climb is 0.6, which for a delta-wing aircraft corresponds to angle of attack $\alpha = 12°$. The engine exhaust is assumed to be inclined at the angle of attack. The modified airplanes have 28% more takeoff thrust than the baseline case. All aircraft must have the same weight as they share the same cruise thrust. The excess takeoff thrust can be used in two fashions: faster velocity at the same climb angle or higher climb angle at the same velocity. Here we consider the latter option. Also, takeoff roll distance is reduced by roughly the amount of

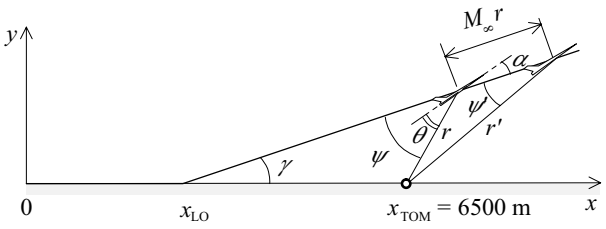

Fig.13 Takeoff flight path with key geometric parameters.

thrust gain. Using well-known relations for takeoff and climb performance [25], the takeoff roll of the modified airplanes is $x_{\rm LO} = 1400$ m and their climb angle is $\gamma = 23°$. Figure 13 shows the generic flight path with key variables.

The takeoff flight speed of all airplanes is 110 m/s ($M_\infty = 0.32$). The cartesian position (x, y) of the airplane is calculated at 0.5-sec intervals from the time of lift off. For each aircraft location, its polar coordinates (r, ψ) relative to the flight path and seen by the takeoff monitor are calculated. Here we distinguish between the apparent (r', ψ') and true (r, ψ) locations of the airplane with regard to sound emission. The apparent location is the actual location of the airplane. The true location is the one from which sound reached the observer. It is easily shown that the true position is at a distance $M_\infty r$ behind the apparent position along the flight path. From the geometry of Fig. 13, the apparent coordinates are

$$r' = \sqrt{y^2 + (x - x_{\rm TOM})^2}$$

$$\psi' = \frac{\pi}{2} - \gamma - \arctan\left(\frac{x - x_{\rm TOM}}{y}\right)$$

and the true coordinates are obtained from

$$r = \frac{r'}{1 - M_\infty^2}\left[-M_\infty \cos\psi + \sqrt{1 - M_\infty^2 \sin^2\psi}\right]$$

$$\sin\psi = \frac{r'}{r}\sin\psi'$$

The polar angle of the exhaust observed by the takeoff monitor is

$$\theta = \psi - \alpha$$

Using these relations, the true distance r and emission angle θ are obtained as functions of time observed by the takeoff monitor.

Data Processing

Following are the steps for processing the laboratory narrowband spectra into perceived noise level:

1. The spectra are corrected to zero absorption using the relations of Ref. [26].

2. The spectra are extrapolated to frequencies higher than those resolved in the experiment (140 kHz) using a decay slope of -30 dB/decade. This is done to resolve the audible spectrum for a full-scale engine. The results are very insensitive on the assumed slope.

3. The spectra are scaled up to engine size by dividing the laboratory frequencies by the scale factor $\sqrt{\mathcal{T}_{\rm eng}/\mathcal{T}_{\rm exp}}$. The full-scale engine diameter is the experimental diameter multiplied by this scale factor.

4. For each observation time t, the scaled-up spectrum corresponding to $\theta(t)$ is obtained. This step requires interpolation between spectra and, for angles outside the range covered in the experiment, moderate extrapolation. To enhance the accuracy of interpolation or extrapolation the spectra are smoothed to remove their wiggles.

5. For each t, the corresponding scaled-up spectrum is corrected for distance and atmospheric absorption. The distance correction is

$$-20\log_{10}\left[\frac{(r/D_p)_{\rm eng}}{(r/D_p)_{\rm exp}}\right]$$

   The absorption correction is applied for ambient temperature 29°C and relative humidity 70% (conditions of least absorption) using the relations of Ref. [26].

6. For each t, the corresponding scaled-up, corrected spectrum is discretized into 1/3-octave bands. The perceived noise level (PNL) is then computed according to the FAR 36 rules [22].

7. The previous step gives the time history of perceived noise level, PNL(t). From it, the maximum level of PNL, PNLM, is determined. The duration of PNL exceeding PNLM-10 dB is calculated and the corresponding "duration correction" is computed according to FAR 36. The effective perceived noise level, EPNL, equals PNLM plus the duration correction. If the duration of PNLM-10 is less than 10 sec the correction amounts to a benefit, otherwise it is a penalty. The duration correction can be very substantial, hence the importance of assessing PNL(t). Our estimate of EPNL does not include the "tone correction", a penalty for excessively protrusive tones in the 1/3-octave spectrum.

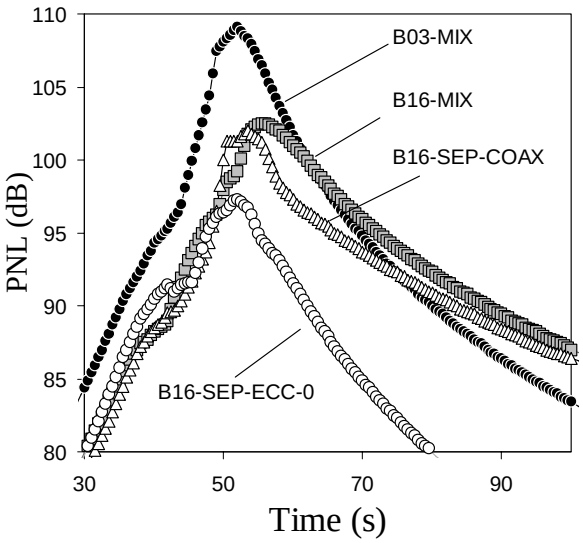

Fig.14 Time history of flyover perceived noise level (PNL) for identical thrusts and flight paths: baseline engine (B03-MIX); modified mixed-flow engine (B16-MIX); modified separate-flow engine with coaxial exhaust (B16-SEP-COAX); and modified separate-flow engine with eccentric exhaust, measured at zero azimuth angle (B16-SEP-ECC-0).

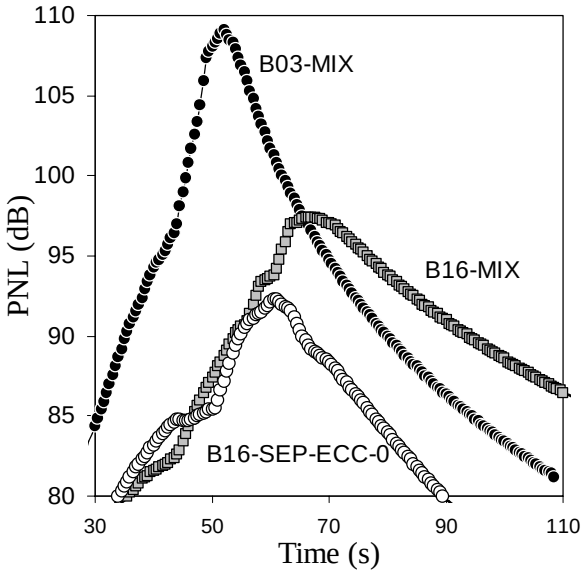

Fig.15 Time history of flyover perceived noise level (PNL) for actual (dissimilar) thrusts and resulting different flight paths: baseline engine (B03-MIX); modified mixed-flow engine (B16-MIX); and modified separate-flow engine with eccentric exhaust, measured at zero azimuth angle (B16-SEP-ECC-0).

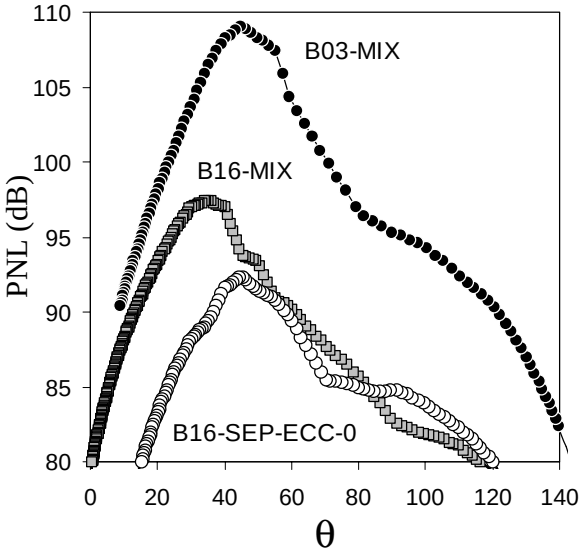

Fig.16 Variation of perceived noise level with emission polar angle observed by takeoff monitor. Curves correspond to the time histories of Fig. 15.

Results

We will compare PNL time histories, and resulting EPNLs, of the baseline and modified airplanes in two ways. One is a realistic comparison that accounts for the better takeoff performance of the modified-engine aircraft. The other is an "academic" comparison in which the flight paths are identical and the engines produce the same thrust. For the latter comparison, we scale down the modified engines so that their thrust equals that of the baseline engine. Obviously the scaled-down engines do not meet the Mach 1.6 cruise requirement, hence the academic nature of this comparison.

Figure 14 compares PNL time histories of aircraft powered by the B03-MIX, B16-MIX, B16-SEP-COAX, and B16-SEP-ECC engines. The flight paths are identical (baseline case) and all engines produce the same thrust, 126 kN. The superiority of the separate-flow, eccentric exhaust is evident. In terms of PNLM, it is 13 dB quieter than the baseline, while the fully-mixed and the coaxial exhausts are 5 dB and 6 dB quieter than the baseline, respectively. EPNL is as follows: 108.5 dB for B03-MIX; 104.0 dB for B16-MIX; 102.5 dB for B16-SEP-COAX; and 98.0 dB for B16-SEP-ECC. In other words, the eccentric separate-flow exhaust gives a 10.5-dB benefit in EPNL, while the mixed-flow and annular exhausts produce only 4.5 db and 6.0 dB benefits, respectively.

Figure 15 makes a more realistic comparison that accounts for the higher thrust of the modified engines and resulting improved takeoff performance. The larger size of the modified engines causes a moderate increase in noise. This is more than counteracted, though, by sound attenuation due to the higher altitude of the aircraft. The PNL histories of B03-MIX (baseline flight path), B16-MIX (enhanced flight path) and B16-SEP-ECC-0 (enhanced flight path) are plotted in the figure. The enhanced takeoff profile produces a 3-3.5 dB attenuation in the sound from the modified aircraft. EPNL is as follows: 108.5 dB for B03-MIX; 101.0 dB for B16-MIX; and 94.5 dB for B16-SEP-ECC-0. A 14-dB reduction in EPNL is thus achievable by using the eccentric separate-flow exhaust.

It is also instructive to plot PNL(t) versus $\theta(t)$ in order to evaluate which range of polar angles is significant to perceived noise. This is done in Fig. 16. First, it is observed that the angles of peak PNL coincide with the angles of peak sound emission as measured in the lab. The aft quadrant ($\theta < 90°$) is clearly very critical to perceived noise. The forward quadrant has limited impact as most of lies below the PNLM-10 threshold.

Concluding Remarks

The possibility of a quiet, fixed-cycle supersonic turbofan engine without mechanical silencers has been explored. The assessment is preliminary and comprises thermodynamic cycle analysis, subscale acoustic measurements, and estimates of effective perceived noise level (EPNL). The approach was to take a typical state-of-the-art military turbofan, increase its bypass ratio from 0.3 to 1.6, and investigate the acoustic and thermodynamic performance of several exhaust configurations. The leading configuration has a separate-flow, eccentric exhaust, which is shown to prevent strong Mach wave radiation towards the ground. An equal-thrust, equal-flight-path comparison shows that the engine with eccentric exhaust it is 10.5 EPNdB quieter than the baseline engine and 6.0 EPNdB quieter than the mixed-flow engine with BPR=1.6. Accounting for the better takeoff performance of an airplane powered by the modified engines, the eccentric exhaust gives a 14-EPNdB benefit relative to the baseline engine. Fuel consumption at Mach 1.6 supersonic cruise is about 3% better than baseline. The modified engines have a fan diameter 37% larger than the baseline engine. This will require careful integration of the engine with the airframe to avoid increases in wave drag due to the larger engine size. Future work will seek optimal nozzle shapes for the primary and secondary flows, a feat that will be facilitated by the rapid-prototyping procedures effected in the UCI lab.

The study does not include the effect of forward flight on acoustics because the UCI lab is not equipped with a tertiary stream. Forward flight is expected to enhance the noise benefit of the eccentric exhaust. Examination of the spectra shows that, except at very low frequencies, noise from the eccentric exhaust is dominated by that of the secondary (bypass) stream (Fig. 7). Forward speed at takeoff will reduce the relative velocity of the bypass stream from 430 to 310 m/s, a 28% drop. Using the simple argument that sound intensity is proportional to $U_{\rm rel}^8$, we expect a noise reduction of 11.5 dB. In contrast, the relative velocity of the mixed-flow exhaust will reduce by only 23% (from 530 to 410 m/s), leading to a noise reduction of 9 dB. These very preliminary arguments suggest that the noise benefit of the separate-flow, eccentric exhaust relative to the mixed-flow exhaust will widen with increasing flight Mach number. Moreover, classical relations for shear-layer growth rate indicate that forward speed will stretch the potential core of the bypass stream more than that of the core stream, yielding better noise shielding of the core stream by the bypass stream. It is hoped that large-scale experiments in government or industry facilities will address these issues.

Acknowledgments

The support by NASA Glenn Research Center is gratefully acknowledged (Grant NAG-3-2345 monitored by Dr. Khairul B. Zaman). Many thanks to Ms. Erin Abbey for her work on rapid prototyping of the jet nozzles and for running the experiments presented here.

References

[1] Smith, M.J.T., "Aircraft Noise", 1st Ed., Cambridge University Press, 1989, pp. 120-134.

[2] Nagamatsu, H.T., Sheer, R.E., and Gill, M.S., "Characteristics of Multitude Multishroud Supersonic Jet Noise Suppressor", *AIAA Journal*, Vol. 10, No. 3, 1972, pp. 307-313.

[3] Tillman, T.G., Paterson, R.W., and Presz, W.M., "Supersonic Nozzle Mixer Ejector", *AIAA Journal of Propulsion and Power*, Vol. 8, No. 2, 1992, pp. 513-519.

[4] Plencner, R.M., "Engine Technology Challenges for the High-Speed Civil Transport Plane", AIAA 98-2505, 1998.

[5] Papamoschou, D., and Debiasi, M., "Directional Suppression of Noise from a High-Speed Jet," *AIAA Journal*, Vol. 39, No. 3, 2001, pp. 380-387.

[6] Troutt, T.R. and McLaughlin, D.K., "Experiments on the Flow and Acoustic Properties of a Moderate Reynolds Number Supersonic Jet", *Journal of Fluid Mechanics*, Vol. 116, March 1982, pp. 123-156.

[7] Tam, C.K.W., Chen, P., and Seiner, J.M., "Relationship Between Instability Waves and Noise of High-Speed Jets", *AIAA Journal*, Vol. 30, No. 7, 1992, pp. 1747-1752.

[8] Tam, C.K.W., and Chen, P., "Turbulent Mixing Noise from Supersonic Jets," *AIAA Journal*, Vol. 32, No. 9, 1994, pp. 1774-1780.

[9] Tam, C.K.W., "Supersonic Jet Noise,", *Annual Review of Fluid Mechanics,* Vol. 27, 1995, pp. 17-43.

[10] Seiner, J.M., Bhat, T.R.S, and Ponton, M.K., "Mach Wave Emission from a High-Temperature Supersonic Jet", *AIAA Journal*, Vol. 32, No. 12, 1994, pp. 2345-2350.

[11] Mitchell, B.E., Lele, S.K., and Moin, P., "Direct Computation of Mach Wave Radiation in an Axisymmetric Supersonic Jet," *AIAA Journal*, Vol. 35, No. 10, 1994, pp. 1574-1580.

[12] Crighton, D.G. and Huerre, P., "Shear-Layer Pressure Fluctuations and Superdirective Acoustic Sources," *Journal of Fluid Mechanics*, Vol. 220, 1990, pp. 355-368.

[13] Avital, E.J., Sandham, N.D, and Luo, K.H., "Mach Wave Radiation in Mixing Layers. Part I: Analysis of the Sound Field," *Theoretical and Computational Fluid Dynamics*, Vol. 12, 1998, pp. 73-90.

[14] Papamoschou, D., "Mach Wave Elimination from Supersonic Jets", *AIAA Journal*, Vol. 35, No. 10, 1997, pp. 1604-1611.

[15] Murakami, E., and Papamoschou, D. "Mixing Layer Characteristics of Coaxial Supersonic Jets," AIAA-2000-2060, 2000.

[16] Rech, J. and Leyman, C., "A Case Study by Aerospatiale and British Aerospace on the Concorde," AIAA Education Series.

[17] Horlock, J.H., Watson, D.T., and Jones, T.V., "Limitations on Gas Turbine Performance Imposed by Large Turbine Cooling Flows," *Journal of Engineering for Gas Turbines and Power*," Vol. 123, July 2001, pp. 487-494.

[18] Debiasi, M., and Papamoschou, D., "Cycle Analysis for Quieter Supersonic Turbofan Engines," AIAA-2001-3749, 2001.

[19] Lord, W.K., MacMartin, D.G., and Tillman, T.G., "Flow Control Opportunities in Gas Turbine Engines," AIAA-2000-2234, 2000.

[20] Guha, A. "Optimum Fan Pressure Ratio for Bypass Engines with Sepataye or Mixed Flow Exhaust Streams," *AIAA Journal of Propulsion and Power,* Vol. 17, No. 5, 2001, pp. 1117-1122.

[21] Kinzie, K.W., and McLaughlin, D.K., "Measurements of Supersonic Helium/Air Mixture Jets," *AIAA Journal,* Vol. 37, No. 11, 1999, pp. 1363-1369.

[22] Federal Aviation Regulations Part 36 - Noise Standards: Aircraft Type and Airwowrthiness Certificiation.

[23] Papamoschou, D., and Debiasi, M. "Noise Measurements in Supersonic Jets Treated with the Mach Wave Elimination Method," *AIAA Journal*, Vol. 37, No. 2, 1999, pp. 154-160.

[24] Ffowcs Williams, J.E., Simson, J., and Virchis, V.J., " Crackle: an Annoying Component of Jet Noise, " *Journal of Fluid Mechanics*, Vol. 71, Part 2, 1975, pp. 251-271.

[25] Shevell, R.S., "Fundamentals of Flight," Prentice Hall, 1989, pp. 265, 293.

[26] Bass, H.E., Sutherland, L.C., Zuckerwar, A.J., Blackstock, D.T., and Hester, D.M., "Atmospheric Absorption of Sound: Further Developments", *Journal of the Acoustical Society of America,* Vol. 97, 1995, pp. 680-683.